International Journal of Technology (2015) 4: 565-572
ISSN 2086-9614 © IJTech 2015

THE EFFECTS OF ANNEALING TEMPERATURE AND SEED LAYER ON THE GROWTH OF ZNO NANORODS IN A CHEMICAL BATH DEPOSITION PROCESS

Amalia Sholehah[1,2], Akhmad Herman Yuwono[1,3*]

[1] *Department of Metallurgical and Materials Engineering, Faculty of Engineering, Universitas Indonesia, Kampus UI Depok, Depok 16424, Indonesia*
[2] *Department Metallurgical Engineering, Faculty of Engineering, University of Sultan Ageng Tirtayasa, Jl. Jend. Sudirman Km 3, Cilegon 42435, Indonesia*
[3] *Tropical Renewable Energy Center (TREC) Faculty of Engineering, Universitas Indonesia, Kampus Baru UI Depok, Depok 16424, Indonesia*

(Received: September 2015 / Revised: September 2015 / Accepted: October 2015)

ABSTRACT

Zinc oxide (ZnO) nanorods have been considered as a potential semiconductor oxide material for the application of dye-sensitized solar cells (DSSC). Various experiments have been conducted to improve its nanostructural characteristics and functional properties in order to make it well suited for enhancing DSSC' performance. Inspired by such studies, the ZnO nanorods array was grown on indium tin oxide ($InSn_2O_3$, ITO) substrate in the present work. For this purpose, a seed solution was prepared at low temperature (0^oC) using zinc nitrate tetrahydrate and hexamethylenetetramine. The ZnO seed layers were deposited onto ITO glass using a spin-coating technique and further annealed at two different temperatures, 200 and 400 ^oC. The seeding was also varied between one, three and five layers, prior to the growing process using the chemical bath deposition method (CBD). The results showed that the annealing temperatures significantly influenced the ZnO nanorods' growth. The optimal condition was achieved by using three seed layers annealed at 200^oC, providing an average diameter of 157.58 nm, the biggest crystallite size (up to 59.63 nm), and a band-gap energy (E_g) of 3.27 eV. Based on the obtained properties, the growth of ZnO nanorods on ITO substrate in this work has the potential to be used for the application of dye-sensitized solar cells.

Keywords: Annealing temperature; Chemical bath deposition; Seed layers; ZnO nanorods

1. INTRODUCTION

Zinc oxide is an important II-VI group oxide semiconductor with various interesting properties. As a direct band gap semiconductor (E_g = 3.34 eV) with a large exciton binding energy of up to 60 meV, ZnO exhibits near-UV emission, transparent conductivity and piezoelectricity. Zinc oxide may exist in many structural configurations that can be easily synthesized from seeding materials. It can also be grown on many different substrates at relatively low temperatures (Anh et al., 2013).

Several previous researches had pointed out that ZnO nanostructures on conductive glass substrates can be used as an excellent anode for DSSC. However, in order to obtain high efficiency, the ZnO nanostructure should be highly ordered and densely covered (Ameen et al., 2011). For this purpose, the seed layers on the conductive glass substrate are required to exist

* Corresponding author's email: ahyuwono@eng.ui.ac.id, Tel. +62-21-786 3510, Fax. +62-21-787 2350
Permalink/DOI: http://dx.doi.org/10.14716/ijtech.v6i4.1948

before the growing process starts. The DSSC anode that was fabricated using non-seeded substrate was known to have an efficiency of around ~0.78 %, while the anode fabricated withseed layers showed trebly improved efficiency (Ameen et al., 2011). Seeded conductive glass substrate can initiate a ZnO nanostructure that is highly uniform with oriented growth (Ameen et al., 2011; Breedon et al., 2009; Yuwono et al., 2010); therefore, the physical properties are improved and the efficiency of the DSSC will be higher. In previous works, ZnO nanorods has been succesfully synthesized on ITO glass using the chemical bath deposition (CBD) technique at low temperature (Adriyanto et al., 2008; Lang et al., 2008; Sholehah et al., 2013), followed by the post-hydrothermal method (Guo et al., 2005; Yuwono et al., 2010; Yuwono et al., 2013). However, the size, orientation and coverage of the ZnO nanorods that are synthesized in these ways still need to be improved. In this research, therefore, the effects of seed layers and annealing temperature on the physical and optical properties of ZnO nanorods were investigated. The correlation among the amount of seed layers, the annealing temperature, and the resulting ZnO nanorods' characteristics were the main interests in this work.

2. METHODOLOGY

Prior to the synthesis process, the ITO glasses were cleaned using aquades, aceton and ethanol in ultrasonic cleaner for 480 seconds. The cleaned glasses were dried and stored in a closed vacuum container until further use. The seeding solution was prepared using 0.05 M zinc nitrate tetrahydrate ($Zn(NO_3)_2.4H_2O$, Merck) and hexamethylenetetramine, HMTA ($C_6H_{12}N_4$, Merck) and dissolved in cold water (0^oC) in a beaker glass. After being aged for one hour, the clear solution was dropped onto ITO glass and left for 10 minutes before the spin-coating process was carried out at 2000 rpm for 20 seconds. Annealing processes were further performed on the coated substrates at 200^oC and 400^oC for 10 minutes in the laboratory oven. This procedure was repeated three and five times with the addition of more seed layers. After being cooled to room temperature, the seeding layers were grown using CBD, whereby the ITO substrates were placed vertically in a beaker glass and heated in the laboratory oven at 90^oC for three hours. For the sake of comparison purposes, samples without seed layers and annealing were also prepared and directly grown by the CBD process.

These substrates were coded as samples O, while those subjected to the seeding procedure with one, three and five layers and annealed at 200^oC were coded as samples 2A, 2B and 2C, respectively. Similar labels were given to samples with one, three and five seed layers but which were annealed at 400^oC, i.e. 4A, 4B, and 4C, respectively. The morphology of the obtained ZnO nanorods was examined using field emission-scanning electron microscopy (FE-SEM, FEI Inspect F-50), while the crystal's structural information was gained using X-ray diffraction (XRD, Pan Analytical X-Pert Pro), and the optical properties were analyzed using diffuse reflectance (DRS) UV-Vis spectroscopy (Shimadzu 2450). The respective E_g of the samples was determined by the Tauc equation (Tauc et al., 1966) on the linear portion of the absorption edges on the spectrum.

3. RESULTS AND DISCUSSION

Figure 1 shows top-view FE-SEM images of substrates without seeding (sample O), and those with one, three and five seed layers and annealed at 200^oC (samples 2A, 2B, and 2C). It can be observed that the samples grew in the nanorods structures with an almost vertical array on the ITO glass substrates with diameters ranging between 120~390 nm, as seen in Table 1. Sample 2A with one seed layer (Figure 1b) provided the largest diameter of ZnO nanorods in comparison to those with three and five layers (Figures 1c, and 1d). It can be seen from Figures 1c and 1d that the addition of more seed layers resulted in a narrower space for the nuclei to grow in the CBD process, and therefore ZnO nanorods with smaller diameters were produced.

It was also found that the addition of more seed layers affected the growth orientation, i.e. the attachment of three and five seed layers on the ITO glass substrate promoted more perpendicular growth of ZnO nanorods. In sample 2A with one seed layer (Figure 1b), it can be seen that the nanorods were not yet suitably oriented, as some still grew in an oblique direction. As a consequence, dissipation in the growing space occured and fewer nanorods could grow on the substrate. The addition of three and five seed layers (Figures 1c, and 1d) resulted in a restricted area for the growth of nanostructures, meaning that more ZnO nanorods with a smaller diameter were present on the substrate; this condition also caused the nanorods to develop in a more vertical array.

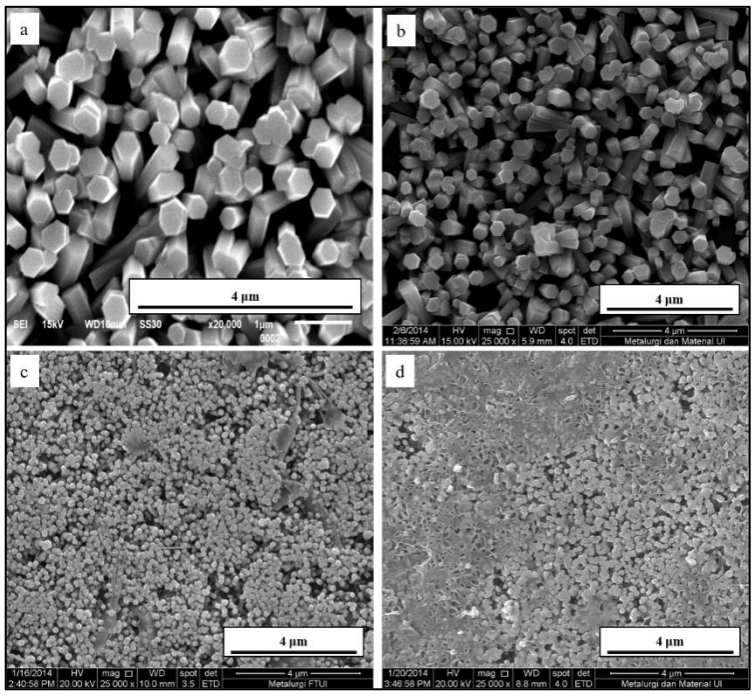

Figure 1 Top-view SEM images of the ZnO nanorods grown by CBD: (a) without annealing and without seed layer (sample O), and after annealing at 200^{o}C and seeding for: (b) one layer (sample 2A), (c) three layers (sample 2B); (d) five layers (sample 2C)

Figures 2b–2c show top-view FE-SEM images of ITO substrates grown by ZnO nanorods that are similar to those shown in Figure 1, but annealed at 400^{o}C (samples 4A, 4B, and 4C). For comparison purposes, the appearance of ZnO nanorods without a seed layer on ITO substrates (sample O) is presented again in Figure 2a. In Figure 2b, some blank spaces on the substrate can be observed, which is assumed to be due to inadequacy during the spin-coating process. However, this condition was addressed by attaching more seed layers. As can be seen in Figure 2c, the addition of three seed layers improved the ZnO nanorods' coverage on the substrate. By further addition of five seed layers (Figure 2d), the void on the ITO surface disappeared and was completely filled with ZnO nanorods. In terms of orientation, the addition of more layers caused the nanorods annealed at 400^{o}C to grow in a similar way to those annealed at 200^{o}C. While the nanorods grown from one seed layer appeared to be in random orientation (Figure 2b), those grown from three and five seed layers (Figures 2c and 2d) were forced to grow in a more perpendicular manner, as a consequence of restricted space in between the ZnO seeds deposited onto the ITO substrates.

The ZnO nanorods' diameter distribution is examined by plotting the frequencies of the various ZnO nanorods' sizes; the results are presented in Figure 3. The average diameters of ZnO nanorod samples at various conditions can be seen in Table 1. By analyzing the curve shape, it

can be clearly seen that sample 2B (three seed layers, annealed at 200^{o}C) is found to have the best size distribution of all the samples. This sample is assumed to have more nanorods that are similarly sized.

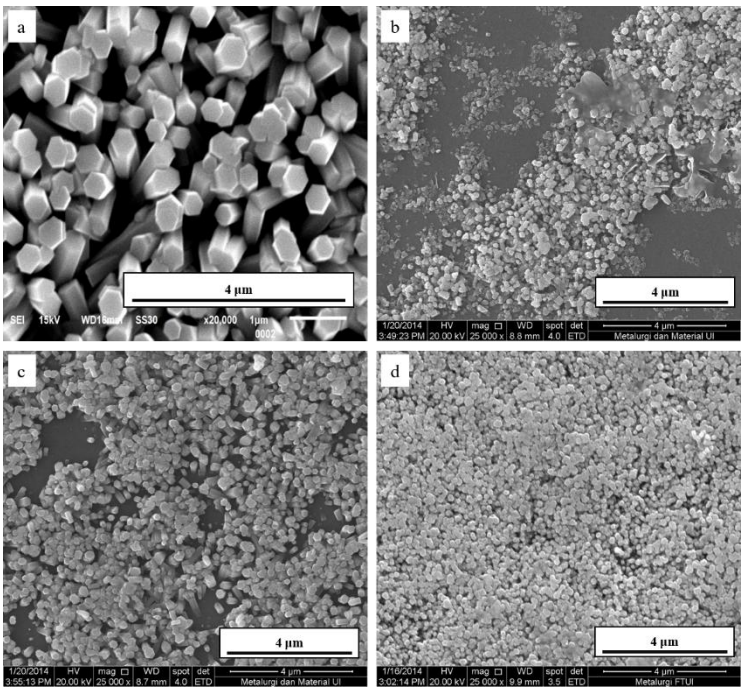

Figure 2 Top-view SEM images of the ZnO nanorods grown by CBD: (a) without annealing and without seed layer (sample O), and after annealing at 400^{o}C and seeding for: (b) one layer (sample 4A); (c) three layers (sample 4B); (d) five layers (sample 4C)

Table 1 The average diameters of ZnO nanorods at various conditions of annealing and seeding

Parameter	Samples						
	O	2A	2B	2C	4A	4B	4C
Average diameter (nm)	325	389.59	157.58	151.52	126.66	184.20	144.49

The crystal structural information of the ZnO nanorod samples was determined by X-ray diffraction, and the resultant diffractogram is presented in Figure 4. Analysis showed that all samples were indicated as the wurtzite phase of ZnO, which matched to JCPDS No. 36-1451. From this figure, it can be seen that all ZnO nanorods were polycrystalline. The most dominant peak is at 2θ~34^{o}, which can be correlated with the crystal plane (002), indicating the growth of nanorods in the –*z*-axis. The high (002) peaks imply that most of the samples grew perpendicularly on the ITO substrate. In this sense, it can be seen that the ZnO nanorods with three layers and annealed at 200^{o}C (sample 2B) had the highest (002) peak. This can be related to the diameter distribution of nanorods, previously shown in Figure 3, where sample 2B was found to have the most evenly shaped diameter distribution curve, as it had the most similarly sized nanorods compared to the other samples. This contributed to the highest crystallinity in the *z*-axis growth orientation. Kenanakis et al. (2009) mentioned that the seed layers were the most important aspect in generating a *z*-axis growth orientation with a controlled diameter.

The crystallite size of the ZnO nanorods was calculated using Scherrer's equation (Venkateswarlu et al., 2010) on the peak broadening of the diffractogram. It should be noted that for the sake of calculation accuracy, broadening that was a result of the non-uniform strain, and the instrumental line width in the XRD apparatus, was excluded. The crystallite sizes of all

ZnO nanorod samples are presented in Table 2. From the table, it can be seen that sample 2B has the largest crystallite size, up to 59.63 nm.

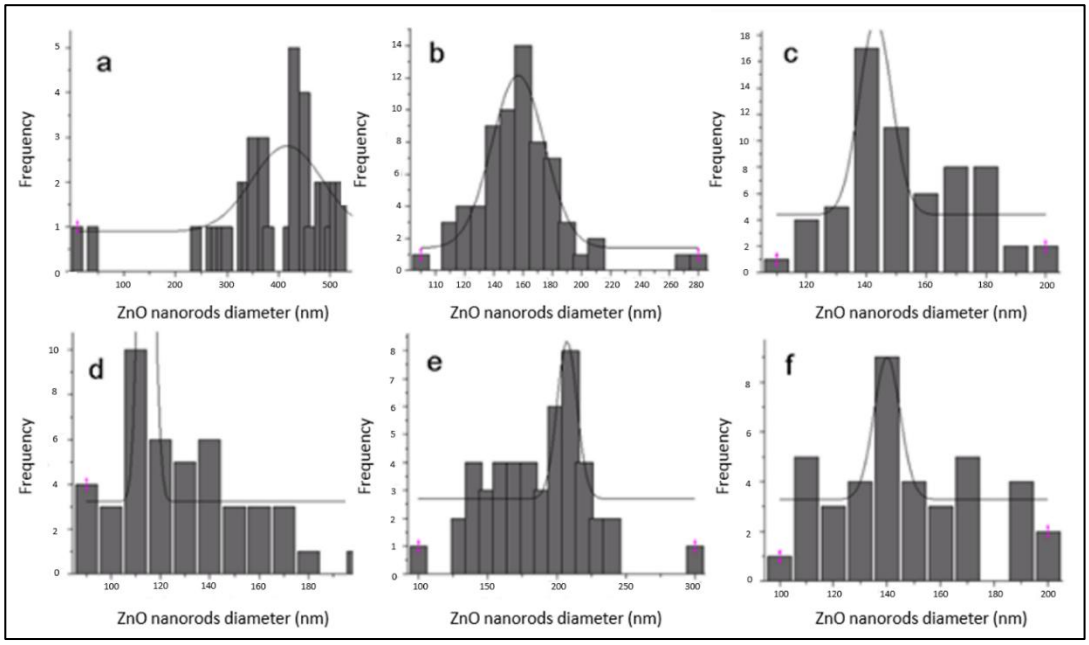

Figure 3 Diameter distribution curves of ZnO nanorods grown by CBD after annealing at 200°C and seeding for: (a) one layer (sample 2A); (b) three layers (sample 2B); (c) five layers (sample 2C), and after annealing at 400°C and seeding for: (d) one layer (sample 4A); (e) three layers (sample 4B); (f) five layers (sample 4C)

Again, the well-distributed diameter of the nanorods is assumed to have an influence on the high crystallinity. It is also interesting to note that most of the ZnO nanorods with seed layers that were attached to the substrate and annealed at 200°C showed an increase in crystallite sizes, in comparison to the as-synthesized ZnO nanorods without seed layers (sample O). However, this is not the case for the nanorod samples annealed at 400°C, whose crystallite sizes decreased the more layers were attached. Further study is in progress to investigate this phenomenon.

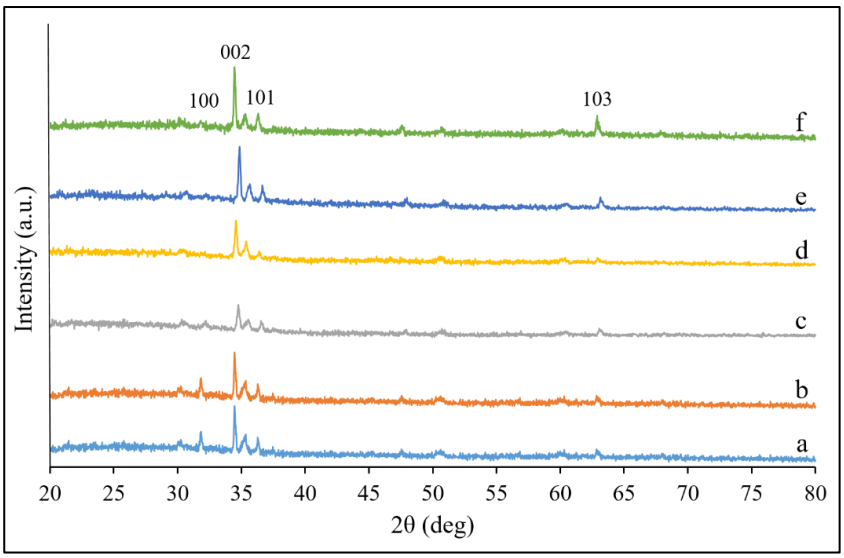

Figure 4 X-ray difractogram of the synthesized ZnO nanorods grown by CBD after annealing at 200°C and seeding for: (a) one layer (sample 2A); (b) three layers (sample 2B); (c) five layers (sample 2C), and

after annealing at 400°C and seeding for: (d) one layer (sample 4A); (e) three layers (sample 4B); (f) five layers (sample 4C)

Table 2 The crystallite size of ZnO nanorods at various conditions of annealing and seeding

Parameter	Samples						
	O	2A	2B	2C	4A	4B	4C
Crystallite size (nm)	22.85	31.17	59.63	28.57	31.90	27.43	18.53

The following figures (Figures 5 and 6) show the results of optical properties study of the synthesized ZnO nanorod samples, using DRS UV-Vis spectroscopy. Inserted in each figure is the Tauc plot of $(\alpha h\nu)^2$ *vs* $(h\nu)$ on the absorbance spectra for estimating the E_g of the samples. The band-gap energy of all ZnO nanorod samples are presented in Table 3. In general, the absorbance spectrums of ZnO nanorods with seed layers show an increase in the wavelength; in other words, they are red-shifted, as compared to the nanorods without seed layers. In samples that were annealed at 200°C, as presented in Figure 5, it can be observed that the absorbance edges fall into quite similar wavelengths. As a consequence, this provides an estimated E_g with similar values for all samples (Table 3), except for sample 2B which is slightly higher (3.27 eV). The thickness of the obtained ZnO seed layers after annealing is presumed to be the important issue here. When applying annealing at 200°C, it is assumed that this process is not sufficient to increase the final thickness of the ZnO nanorods layers, even when the previous seeding procedure is repeated up to three or five times. Meanwhile, when annealing at 400°C was carried out on the seeded samples, the absorbance peaks show a wavelength decrease (they are blue-shifted) as more seed layers were attached to the ITO substrates (Figure 6). With an absorbance edge of shorter wavelength, the estimated band gap energy (E_g) is indeed found to be higher. This blue-shift condition confirms the crystallite growth, as determined by previous XRD analysis and presented in Table 2. In the nanometer regime, the crystallite size of semiconductor nanostructures significantly affects the band gap energy, where the smaller the nanocrystallite size, the bigger the band gap.

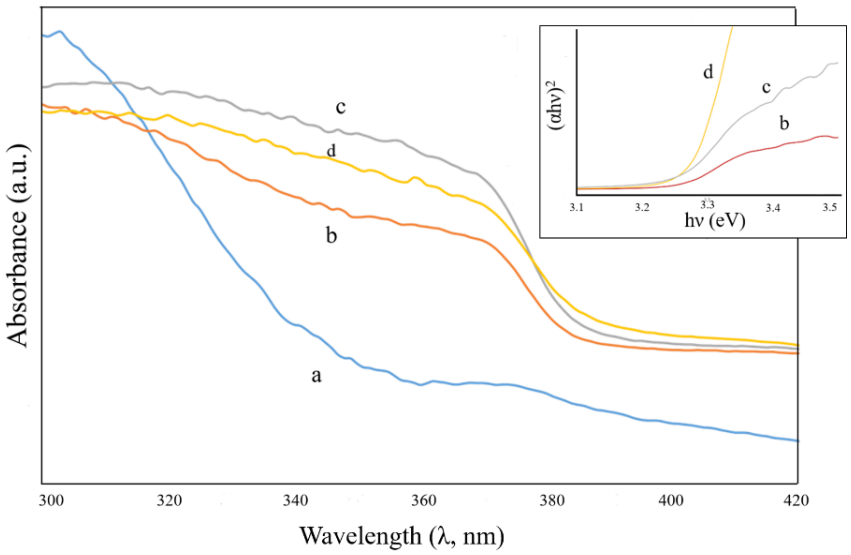

Figure 5 Absorbance spectrums of ZnO nanorods grown by CBD: (a) without seed layer (sample O), and after annealing at 200°C and seeding for: (b) one layer (sample 2A); (c) three layers (sample 2B); (d) five layers (sample 2C). Inserted figure is the Tauc plot of all synthesized ZnO nanorods with seed layers and annealed at 200°C

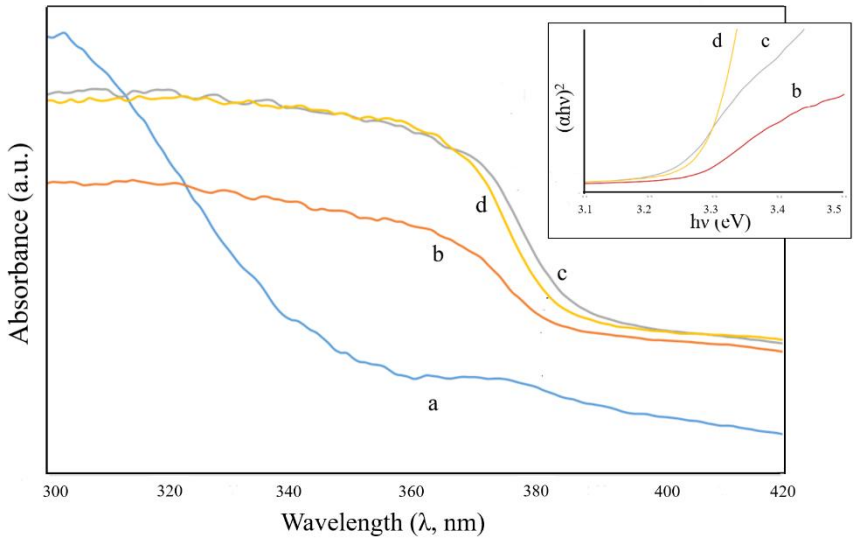

Figure 6 Absorbance spectrums of ZnO nanorods grown by CBD: (a) without seed layer (sample O), and after annealing at 400°C and seeding for: (b) one layer (sample 2A); (c) three layers (sample 2B); (d) five layers (sample 2C). Inserted is the Tauc plot of all synthesized ZnO nanorods with seed layers and annealed at 400°C

Table 3 The band gap energy of ZnO nanorods at various conditions of annealing and seeding

Parameter	Samples						
	O	2A	2B	2C	4A	4B	4C
Band gap energy, E_g (eV)	3.63	3.26	3.27	3.26	3.25	3.27	3.29

By applying seed layers to the ITO substrate, it can be concluded that the properties of ZnO nanorods improved. Zinc oxide nanorods with annealed seed layers had a smaller diameter as a result of the narrower space for ZnO growth on the substrate. The addition of seed layers also improved the orientation of the ZnO nanorods array. As a result, with a more oriented structure, the crystallinity is higher and the band-gap energy is lower. The decrease in band-gap energy is due to the restrained exciton bands and the increase in exciton intensity. This can improve the energy absorption in visible wavelengths (Ye & Chen, 2012).

4. CONCLUSION

Vertically aligned ZnO nanorods on ITO substrates were successfully synthesized using the CBD method, assisted by seeding and annealing treatments. The seed layers were proven to provide some improvements in the ZnO nanorods' characteristics. The optimal condition was obtained by applying three seed layers and annealing at 200°C, with a resulting average diameter, crytallite size and band-gap energy of 157.58 nm, 59.63 nm, and 3.27 eV, respectively. The ZnO nanorods obtained in this study have the potential to be used as the semiconductor oxide layer in DSSC.

5. ACKNOWLEDGEMENT

The authors would like to thank the Ministry of Research, Technology and Higher Education, Republic of Indonesia, as well as the Directorate of Research and Community Services, Universitas, Indonesia, for the financial support of this project through Hibah Penelitian

Unggulan Perguruan Tinggi (PUPT) 2015 with contract number 0549 /UN2.R12/HKP.05.00/2015, and would also like to thank the University of Sultan Ageng Tirtayasa for its support through Hibah Penelitian Disertasi Doktor, with contract number 448/UN43.9/PL/K/2014.

6. REFERENCES

Adriyanto, F., Sze, P., Wang, Y., 2008. ZnO Nanorods on Plastic Substrate from Zinc Nitrate Hexahydrate and Hexamethylenetetramine Solution. In: *Proceedings of the 9th International Conference on Solid-State and Integrated-Circuit Technology*, pp. 2–5. Beijing, China: IEEE

Ameen, S., Akhtar, M.S., Kim, Y.S., Yang, O.B., Shin, H.S., 2011. Influence of Seed Layer Treatment on Low Temperature Grown ZnO Nanotubes: Performances in Dye Sensitized Solar Cells. *Electrochimica Acta*, Volume 56(3), pp. 1111–1116

Anh, V., Anh, L., Quang, T., Ngoc, V., Quy, N.V., 2013. Applied Surface Science Enhanced NH_3 Gas Sensing Properties of a QCM Sensor by Increasing the Length of Vertically Orientated ZnO Nanorods. *Applied Surface Science*, Volume 265, pp. 458–464

Breedon, M., Rix, C., Kalantar-zadeh, K., 2009. Seeded Growth of ZnO Nanorods from NaOH Solutions. *Materials Letters*, Volume 63(2), pp. 249–251

Guo, M., Diao, P., Cai, S., 2005. Hydrothermal Growth of Perpendicularly Oriented ZnO Nanorod Array Film and its Photoelectrochemical Properties. *Applied Surface Science*, Volume 249(1–4), pp. 71–75

Kenanakis, G., Vernardou, D., Koudoumas, E., Katsarakis, N., 2009. Growth of C-axis Oriented ZnO Nanowires from Aqueous Solution: The Decisive Role of a Seed Layer for Controlling the Wires' Diameter. *Journal of Crystal Growth*, Volume 311(23-24), pp. 4799–4804

Lang, J., Yang, J., Li, C., Yang, L., Han, Q., Zhang, Y., Liu, X., 2008. Synthesis and Optical Properties of ZnO Nanorods. *Crystal Research and Technology*, Volume 43(12), pp. 1314–1317

Sholehah, A., Herman, A., Poespawati, N.R., Trenggono, A., Maulidiah, F., 2013. High Coverage ZnO Nanorods on ITO Substrates via Modified Chemical Bath Deposition (CBD) Method at Low Temperature. *Advanced Materials Research*, Volume 789, pp. 151–156

Tauc, J., Grigorovici, R., Vancu, A., 1966. Optical Properties and Electronic Structure of Amorphous Germanium. *Physica Status Solidi (b)*, Volume 15(2), pp. 627–637

Venkateswarlu, K., Chandra-Bose, A., Rameshbabu, N., 2010. X-ray Peak Broadening Studies of Nanocrystalline Hydroxyapatite by Williamson–Hall Analysis. *Physica B: Condensed Matte*r, Volume 405(20), pp. 4256–4261

Ye, N., Chen, C.C., 2012. Investigation of ZnO Nanorods Synthesized by a Solvothermal Method, using Al-doped ZnO Seed Films. *Optical Materials*, Volume 34(4), pp. 753–756

Yuwono, A.H., Munir, B., Ferdiansyah, A., Rahman, A., Handini, W., 2010. Dye Sensitized Solar Cell with Conventionally Annealed and Post-hydrothermally Treated Nanocrystalline Semiconductor Oxide TiO_2 Derived from Sol Gel Process. *Makara Journal Teknologi*, Volume 14(2), pp. 53–60

Yuwono, A.H., Sholehah, A., Harjanto, S., Dhaneswara, D., Maulidiah, F., 2013. Optimizing the Nanostructural Characteristics of Chemical Bath Deposition Derived ZnO Nanorods by Post-hydrothermal Treatments. *Advanced Materials Research*, Volume 789, pp. 132–137